Journal of Alloys and Compounds 506 (2010) 428–433

Contents lists available at ScienceDirect

Journal of Alloys and Compounds

journal homepage: www.elsevier.com/locate/jallcom

Complete set of elastic, dielectric, and piezoelectric coefficients of [−1 0 1] poled $0.23Pb(In_{1/2}Nb_{1/2}O_3)$–$0.45Pb(Mg_{1/3}Nb_{2/3})O_3$–$0.32PbTiO_3$ single crystals

Da'an Liu[a,b,*], Yaoyao Zhang[a,b], Wei Wang[a,b], Bo Ren[a,b], Qinhui Zhang[a,b], Jie Jiao[a,b], Xiangyong Zhao[a], Haosu Luo[a]

[a] Key Laboratory of Inorganic Functional Material and Device, Shanghai Institute of Ceramics, Chinese Academy of Sciences, Shanghai 201800, China
[b] Graduate School of the Chinese Academy of Sciences, Beijing 100049, China

ARTICLE INFO

Article history:
Received 15 April 2010
Received in revised form 2 July 2010
Accepted 6 July 2010
Available online 14 July 2010

Keywords:
PIN–PMN–PT
Single crystals
Piezoelectric properties

ABSTRACT

In order to better utilize the superior transverse and shear piezoelectric properties of $0.23Pb(In_{1/2}Nb_{1/2}O_3)$–$0.45Pb(Mg_{1/3}Nb_{2/3})O_3$–$0.32PbTiO_3$ single crystals near the morphotropic phase boundary, a complete set of elastic, dielectric, and piezoelectric coefficients of [$\bar{1}$ 0 1] poled single crystal were determined by resonance and ultrasonic methods at room temperature. The electromechanical coupling coefficient k_{32} and transverse piezoelectric coefficient d_{32} can reach 0.94 and −2073 pC/N, respectively. At the same time, electromechanical coupling coefficient k_{15} and shear piezoelectric constant d_{15} are as high as 0.91 and 2526 pC/N. This complete set of material properties will provide convenience for device designs and fundamental theoretical studies such as applications in high-sensitivity medical ultrasonic transducers and large displacement actuators.

© 2010 Elsevier B.V. All rights reserved.

1. Introduction

In recent years, $(1-x)Pb(Mg_{1/3}Nb_{2/3})O_3$–$xPbTiO_3$ (PMNT) and $(1-y)Pb(Zn_{1/3}Nb_{2/3})O_3$–$yPbTiO_3$ (PZNT) relaxor based ferroelectric single crystals have attracted much attention [1–4]. There have been many research efforts in developing some novel piezoelectric ceramics with perovskite structure by a new approach, such as: Pb(Fe,W)–$PbTiO_3$ [5], $Pb(Mg,Nb)O_3$ [6], $Pb(Mg,Nb)O_3$–$PbTiO_3$ [7] and $Pb(Mg,Nb)O_3$–$Pb(Zn,Nb)O_3$–$Pb(Zr,Ti)O_3$ [8]. Liquid-phase sintering mechanism may take partial effect in the densification of PIN–PMN–PT ceramics due to the round grain morphology. Also, similar system ceramics with liquid-phase are reported in literature [9–14]. However, some issues remain to be improved, such as the low piezoelectric coefficient for ceramics, low depoling temperature and coercive field for many crystals. So far, the most successful choice is the ternary compound $xPb(In_{1/2}Nb_{1/2})O_3$–$(1-x-y)Pb(Mg_{1/3}Nb_{2/3})O_3$–$yPbTiO_3$ (xPIN-$(1-x-y)$PMN–yPT or PIN–PMN–PT) system. After being poled along the <0 0 1> direction, the piezoelectric coefficient d_{33} and electromechanical coupling coefficient k_{33} of PIN–PMN–PT single crystals near the morphotropic phase boundary (MPB) composition could reach as high as 1320 pC/N and 0.91 [15], respectively, much higher than that of ceramics (24PIN–42PMN–34PT ceramics: $d_{33} \sim 496$ pC/N, $k_{33} \sim 0.72$) [16].

PIN–PMN–PT system is more attractive compared to the PMNT system for its wider temperature range in application. The results show that the PIN–PMN–PT single crystals have a higher phase transition temperature T_{R-T} (ferroelectric rhombohedral phase to tetragonal phase transition) than those of many other crystals (PIN–PMN–PT $T_{R-T} > 100\,^{\circ}C$, PMNT T_{R-T}: 60–90 °C, Curie temperature PIN–PMN–PT $T_C > 160\,^{\circ}C$, PMNT T_C: 120 ∼ 150 °C) with comparable piezoelectric properties near MPB [17,18]. High-quality PIN–PMN–PT single crystals have already been grown by the modified Bridgman method [19,20]. In this literature, the ultra-high transverse and shear piezoelectric properties are obtained when being poled along [$\bar{1}$ 0 1]. Therefore, it is promising for us to apply these superior piezoelectric properties of [$\bar{1}$ 0 1] poled PIN–PMN–PT single crystals to many kinds of transducers, such as piezoelectric transformers, ultrasonic transducers and actuators [21,22].

2. Experimental

Samples of 0.23PIN–0.45PMN–0.32PT single crystals were prepared for electromechanical characterization on the order of Φ 50 mm × 80 mm, and the obtained crystal boule is shown in Fig. 1. Seven cut-type samples with main parallel surfaces were prepared for measuring the properties as seen in Fig. 2, which were oriented along the [1 0 1]/[$\bar{1}$ 0 1]/[0 1 0] directions possessing appropriate aspect ratios as determined by IEEE standards [23]. The dimensions of two samples for thickness shear mode vibration satisfy 14:7:1, and for the length-extensional resonance measurements, the aspect ratio of the resonators should exceed 5:1 in order to yield nearly pure resonance modes. The samples were poled along [$\bar{1}$ 0 1] in the

* Corresponding author at: Key Laboratory of Inorganic Functional Material and Device, Shanghai Institute of Ceramics, Chinese Academy of Sciences, Shanghai 201800, China. Tel.: +86 21 69987759; fax: +86 21 59927184.
E-mail address: liudaan123@hotmail.com (D. Liu).

0925-8388/$ – see front matter © 2010 Elsevier B.V. All rights reserved.
doi:10.1016/j.jallcom.2010.07.021

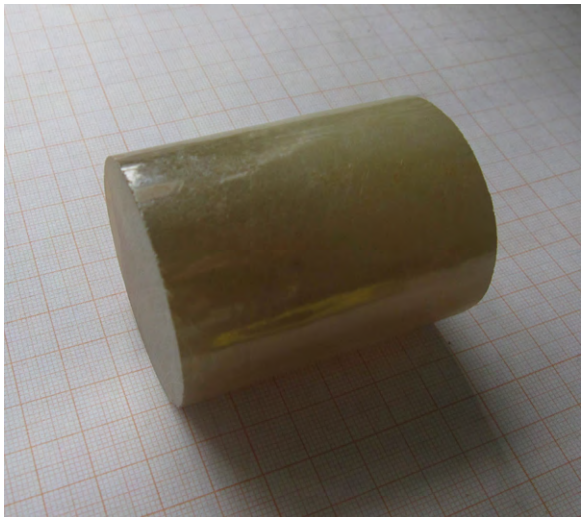

Fig. 1. A photo of 0.23PIN–0.45PMN–0.32PT single crystal with 50 mm diameter.

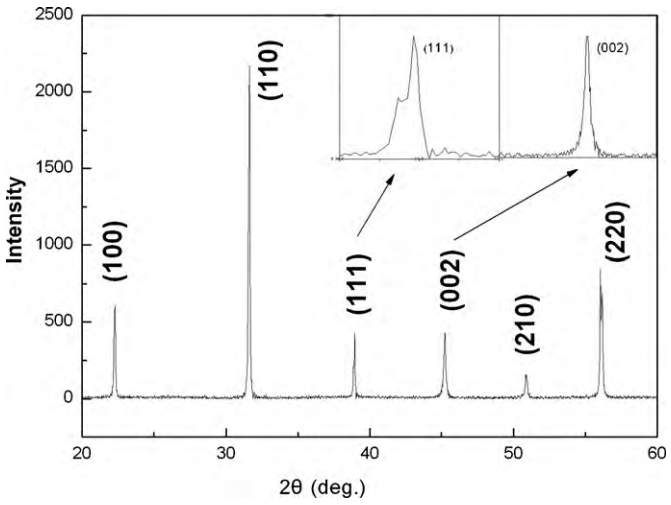

Fig. 3. XRD patterns of the 0.23PIN–0.45PMN–0.32PT single crystals at room temperature.

silicon oil under an electric field of 10 kV/cm for 15 min at 130 °C. The density ρ was determined from the Archimedes principles. For the resonance and antiresonance frequencies of the resonators, a Precision Impedance Analyzer (Agilent 4294 A) was employed. A 15 MHz longitudinal transducer and a 20 MHz shear wave transducer (Panametrics) were used for the ultrasonic measurements. The combined ultrasonic and resonance technique offers much better accuracy in the full matrix property characterization, for the ultrasonic measurement can provide a check on some parameters, such as c_{33}^D, c_{55}^E.

3. Results and discussion

At room temperature, the 0.23PIN–0.45PMN–0.32PT single crystals present a rhombohedral structure with crystal symmetry (*3m*), which can be proved from the XRD pattern (Fig. 3). Fig. 4(a) shows the spontaneous polarization which is along one of the eight <1 1 1> directions of cubic coordinates in each unit cell. After being poled along [$\bar{1}$ 0 1], there are two remaining energetic degenerate dipole orientations (Fig. 4(b)), and the macroscopic symmetry is changed to orthorhombic *mm2* [24,25]. We take the poling direction as the 3 direction, which is along [$\bar{1}$ 0 1] of the cubic coordinates, and the [1 0 1] and [0 1 0] are defined as the 1 and 2 directions, respectively. For the orthorhombic symmetry, there are a total of 17 independent electroelastic constants: three dielectric constants, nine elastic constants, and five piezoelectric constants to be determined, while [0 0 1] poled crystals have *4mm* macroscopic symmetry and only 11 independent constants.

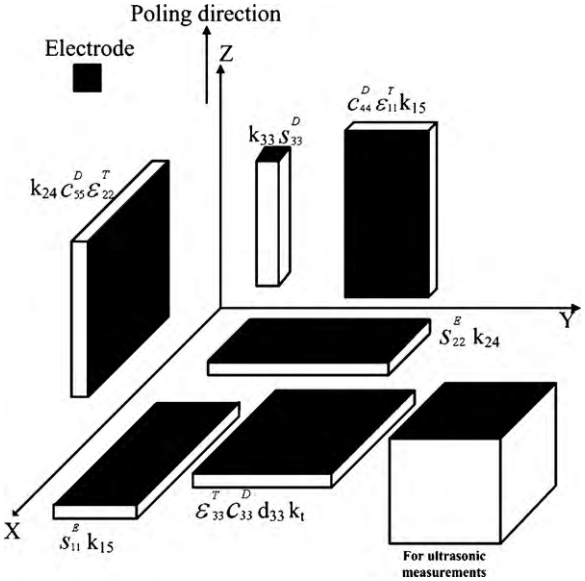

Fig. 2. Seven type samples used to determine the whole set of physical property data of 0.23PIN–0.45PMN–0.32PT single crystals.

From the resonance and antiresonance frequencies we can calculate corresponding piezoelectric coefficients d_{31}, d_{32} and d_{33}, the elastic compliance s_{11}^E, s_{22}^E, s_{33}^E, and s_{44}^E and the elastic stiffness c_{33}^D. The free and clamped permittivity ε_{11}^T, ε_{33}^T, ε_{11}^S and ε_{33}^S were calculated from the low (1 kHz) and high frequency($\sim 2f_a$) capacitances using the parallel capacitor approximation.

Piezoelectric coefficients e_{33}, e_{31}, and elastic constants s_{12}^E, s_{13}^E, c_{33}^E, can be counted from the equations:

$$e_{33} = k_t\sqrt{c_{33}^D\varepsilon_{33}^S} \tag{1}$$

$$e_{31} = \frac{\varepsilon_{33}^T - \varepsilon_{33}^S - d_{33}e_{33}}{2d_{31}} \tag{2}$$

$$s_{13}^E = \frac{d_{33} - e_{33}s_{33}^E}{2e_{31}} \tag{3}$$

$$s_{12}^E = -s_{11}^E + \frac{2(s_{13}^E)^2}{s_{33}^E - 1/c_{33}^E} \tag{4}$$

$$c_{33}^E = c_{33}^D(1 - k_t^2) \tag{5}$$

The basic relationships to calculate c_{11}^E, c_{22}^E, s_{23}^E from the measured data are:

$$c_{11}^E = \frac{s_{22}^E - (s_{23}^E)^2}{S} \tag{6}$$

$$c_{22}^E = \frac{s_{11}^E s_{33}^E - (s_{13}^E)^2}{S} \tag{7}$$

$$c_{33}^E = \frac{s_{11}^E s_{22}^E - (s_{12}^E)^2}{S} \tag{8}$$

where $S = s_{11}^E\left(s_{22}^E s_{33}^E - \left(s_{23}^E\right)^2\right) - s_{12}^E\left(s_{12}^E s_{33}^E - s_{13}^E s_{23}^E\right) + s_{13}^E\left(s_{12}^E s_{23}^E - s_{13}^E s_{22}^E\right)$. Considering the orthorhombic *mm2* symmetry, with the formula:

$$s_{\phi\gamma}^D = s_{\phi\gamma}^E - d_{\eta\phi}d_{\mu\gamma}\beta_{\eta\mu}^T \tag{9}$$

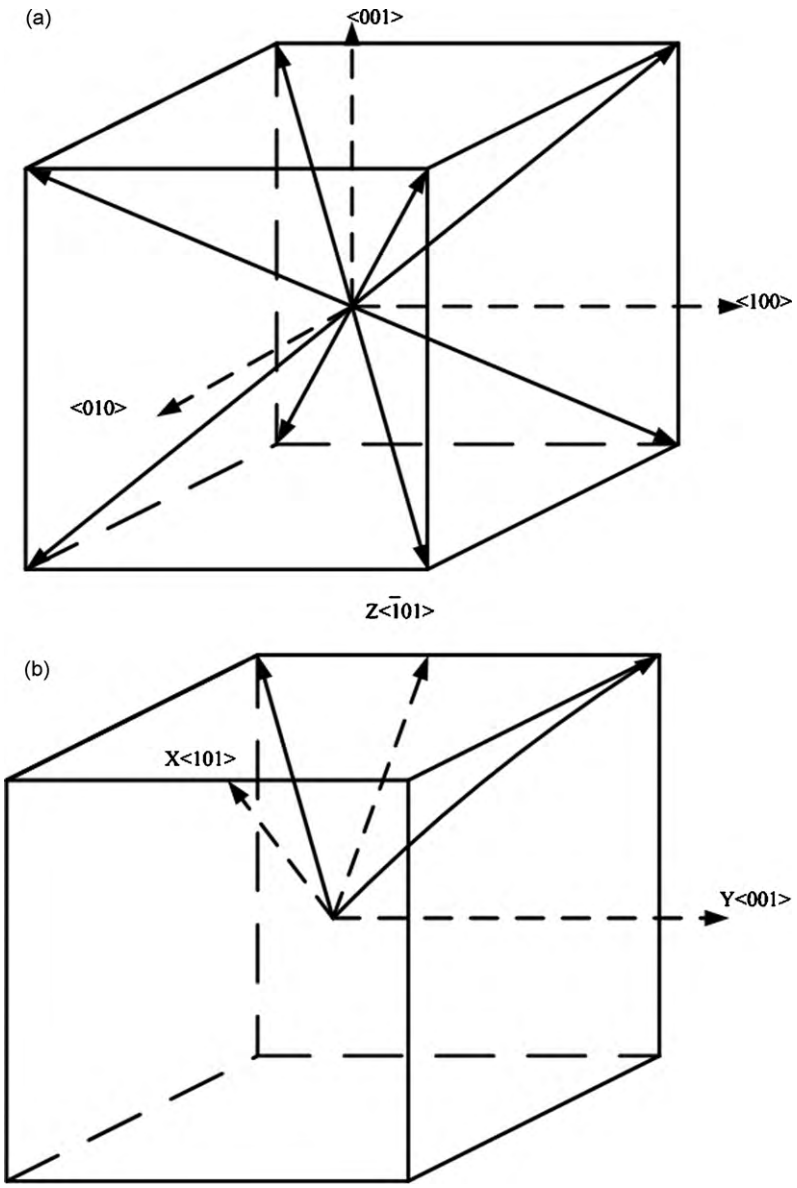

Fig. 4. (a) Spontaneous polarization along eight {1 1 1} directions of cubic phase in unpoled 0.23PIN–0.45PMN–0.32PT single crystals. (b) Two remaining polarization in [$\bar{1}$01] poled PIN–PMN–PT single crystals.

nearly all the s_{ij}^E, c_{ij}^E, s_{ij}^D, c_{ij}^D (except s_{66}^E, c_{66}^E, s_{66}^D, c_{66}^D) can be determined from the matrix inversion:

$$\left[c_{ij}^E\right] = \left[s_{ij}^E\right]^{-1} \tag{10}$$

$$\left[s_{ij}^D\right] = \left[c_{ij}^D\right]^{-1} \tag{11}$$

Then, the rest piezoelectric constants can be derived according to the formula:

$$e_{\alpha\beta} = d_{\alpha\chi} c_{\chi\beta}^E \tag{12}$$

For [$\bar{1}$ 0 1] poled crystals symmetry has more independent constants than [0 0 1] poled, there are not enough equations to calculate s_{66}^E, c_{66}^E, s_{66}^D and c_{66}^D. As a supplement, measuring phase velocities with ultrasonic transducers is used to obtain c_{66}^E, and then s_{66}^E, s_{66}^D, c_{66}^D can be calculated from the equations above.

The results in Fig. 5 show the resonance and antiresonance characteristics of impedance and phase for the six cut-type [$\bar{1}$ 0 1] poled crystals at room temperature. Then based on the above calculation process, with the ultrasonic measurements to confirm the rest data, a complete set of elastic, dielectric, and piezoelectric coefficients of [$\bar{1}$ 0 1] poled PIN–PMN–PT single crystal were obtained, as shown in Table 1.

The full matrix data allow us to comprehensively evaluate the [$\bar{1}$ 0 1] direction poled multidomain crystal and compare the properties with that of [0 0 1] poled crystals. These properties are quite different from those of [0 0 1] poled PIN–PMN–PT. For example, the piezoelectric coefficient d_{15} of [$\bar{1}$ 0 1] poled crystal is 2526 pC/N, and the d_{24} is only 62 pC/N; while for [0 0 1] poled system, d_{15} and d_{24} are the same, which is only 232 pC/N [27]. It is worth mentioning that the shear and transverse properties are very large in the [$\bar{1}$ 0 1] poled PIN–PMN–PT crystals. The elastic compliance constants s_{22}^E and s_{44}^E, with the same trend of d_{32} and d_{15}, respectively, have very large values of 112.36×10^{-12} and 163.42×10^{-12} m^2/N, which significantly exceed that of many other crystals of the elastic compliance data.

The largest improvement compared to [0 0 1] poled PIN–PMN–PT are the d_{32} and d_{15}, which can reach −2073 and 2526 pC/N, respectively. And with all these constants determined, the piezoelectric constants and electromechani-

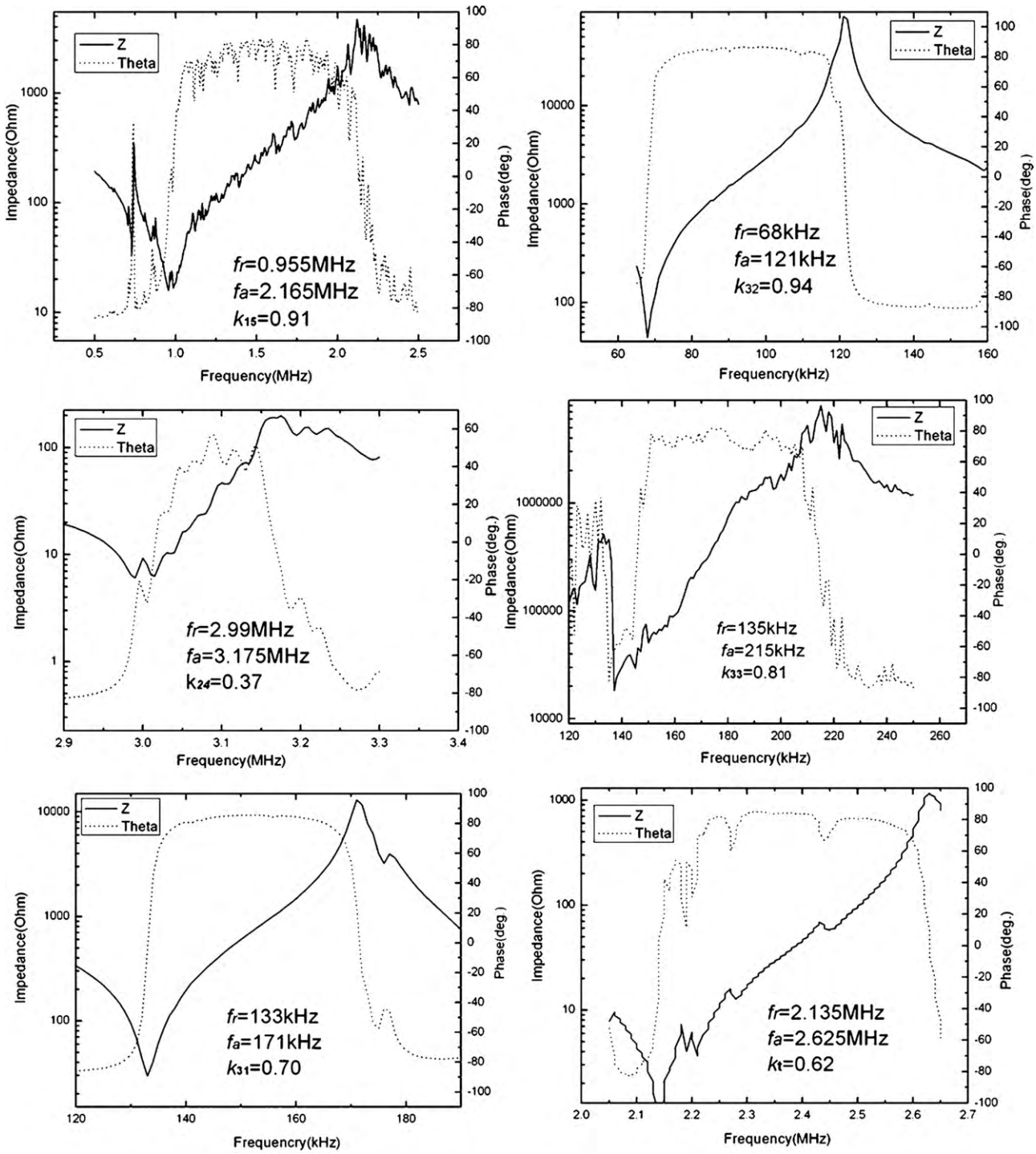

Fig. 5. Impedance and phase characteristics for six-cut type samples at room temperature.

cal coupling coefficients comparison of three kinds of single crystals (PZNT7% [28], PMNT29% [4], 0.23PIN–0.45PMN–0.32PT) in hot research recently can be achieved in Table 2. The electromechanical coupling coefficients of 0.23PIN–0.45PMN–0.32PT ($k_{15} \sim 0.91$, $k_{32} \sim 0.94$) are very impressive, much larger than that of reported [0 1 1] poled PZNT7% ($k_{15} \sim 0.40$, $k_{32} \sim 0.86$) crystals.

The temperature dependence of the dielectric constant $\varepsilon_{33}^{T}/\varepsilon_0$ of the [$\bar{1}$ 0 1] poled 0.23PIN–0.45PMN–0.32PT and [1 1 0] poled PMNT29% single crystals, with the compositions both near MPB, are compared in Fig. 6. Unlike [0 0 1] poled crystals, three ferroelectric phase transitions are shown for <110> poled samples. Due to some results on dielectric properties before [17,26], the two ferroelectric phase transition temperatures of PIN–PMN–PT crystal observed below its Curie temperature ($T_C \sim 171\,^{\circ}C$) can be confirmed to be rhombohedral to orthorhombic phase transition $T_{R-O} \sim 110\,^{\circ}C$ and orthorhombic to tetragonal phase transition $T_{O-T} \sim 118\,^{\circ}C$. Compared to [1 1 0] poled PMNT near the MPB composition, the T_{R-O}, T_{O-T}, and T_C of [$\bar{1}$ 0 1] poled PIN–PMN–PT increased by 33, 23, and 36 °C, respectively. Therefore, the addition of lead indium niobate can obviously enhance the phase transition temperature.

Table 1
Complete set of electromechanical coefficients of [$\bar{1}$ 0 1] poled 0.23PIN–0.45PMN–0.32PT single crystals (density ρ = 8440 kg/m^3).

Elastic stiffness constants: c_{ij} (10^{10} N/m^2)

c^E_{11}	c^E_{12}	c^E_{13}	c^E_{22}	c^E_{23}	c^E_{33}	c^E_{44}	c^E_{55}	c^E_{66}	c^D_{11}	c^D_{12}	c^D_{13}	c^D_{22}	c^D_{23}	c^D_{33}	c^D_{44}	c^D_{55}	c^D_{66}
7.12	0.94	3.64	3.48	6.08	14.57	0.61	29.33	4.25	5.36	8.57	2.50	−3.77	1.41	11.58	3.72	34.01	4.25

Elastic compliance constants s_{ij} (10^{-12} m^2/N)

s^E_{11}	s^E_{12}	s^E_{13}	s^E_{22}	s^E_{23}	s^E_{33}	s^E_{44}	s^E_{55}	s^E_{66}	s^D_{11}	s^D_{12}	s^D_{13}	s^D_{22}	s^D_{23}	s^D_{33}	s^D_{44}	s^D_{55}	s^D_{66}
17.09	−10.52	8.66	112.36	−49.53	29.7	163.42	3.41	23.53	8.72	18.32	−4.11	13.08	−5.55	10.20	26.87	2.94	23.53

Piezoelectric constants d(10^{-12} C/N)

d_{15}	d_{24}	d_{31}	d_{32}	d_{33}
2526	62	602	−2073	918

Electromechanical coupling coefficients k

k_{15}	k_{24}	k_{31}	k_{32}	k_{33}	k_t
0.91	0.37	0.70	0.94	0.81	0.62

Piezoelectric constants e(C/m^2)

e_{15}	e_{24}	e_{31}	e_{32}	e_{33}
740.88	0.38	13.61	−10.67	29.63

Piezoelectric constants g(10^{-3} Vm/N)

g_{15}	g_{24}	g_{31}	g_{32}	g_{33}
53.54	7.57	13.91	47.91	21.22

Piezoelectric constants h(10^8 V/m)

h_{15}	h_{24}	h_{31}	h_{32}	h_{33}
19.92	25.75	97.97	−18.41	51.11

Relative dielectric constants ε(ε_0)

ε^S_{11}	ε^S_{22}	ε^S_{33}	ε^T_{11}	ε^T_{22}	ε^T_{33}
829	1345	655	5331	925	4889

Relative dielectric constants β($10^{-4}/\varepsilon_0$)

β^S_{11}	β^S_{22}	β^S_{33}	β^T_{11}	β^T_{22}	β^T_{33}
12.06	7.43	15.27	1.88	10.81	2.05

Table 2
Measured electromechanical coupling coefficients k_{ij} and piezoelectric coefficients d_{ij}(pC/N) for <1 1 0> poled PZNT7% single crystals, PMNT29% single crystals, and 0.23PIN–0.45PMN–0.32PT single crystals.

Compositions	k_{15}	k_{24}	k_{31}	k_{32}	k_{33}	k_t	d_{15}	d_{24}	d_{31}	d_{32}	d_{33}
PZNT7% [28]	0.40	0.10	0.35	0.86	0.87	0.19	1823	50	478	−1460	1150
PMNT29% [4]	0.83	0.35	0.76	0.94	0.78	0.48	1188	167	610	−1883	1020
0.23PIN–0.45PMN–0.32PT	0.91	0.37	0.70	0.94	0.81	0.62	2526	62	602	−2073	918

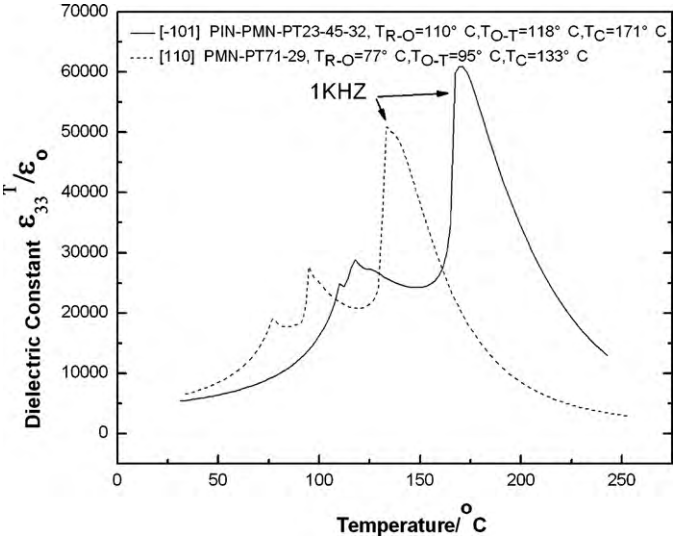

Fig. 6. The temperature dependence of the dielectric constant $\varepsilon^T_{33}/\varepsilon_0$ of the [$\bar{1}$01] poled 0.23PIN–0.45PMN–0.32PT and [1 1 0] poled PMNT29% single crystals.

4. Conclusions

In summary, we have grown 0.23PIN–0.45PMN–0.32PT single crystals near the MPB composition by a modified Bridgman method and obtained a complete set of elastic, dielectric, and piezoelectric coefficients of [$\bar{1}$ 0 1] poled single crystals by combined resonance and ultrasonic methods. It reveals superior transverse piezoelectric properties, with d_{32} and k_{32} as high as −2073 pC/N and 0.94. On the other hand, the large shear mode properties ($k_{15} \sim 0.91$, $d_{15} \sim 2526$ pC/N) are also attractive in application of shear transducer and vibration energy harvesting devices. Moreover, the T_{R-O}, T_{O-T}, and T_C of [$\bar{1}$ 0 1] poled PIN–PMN–PT are all more than 23 °C higher compared to those of PMNT crystals, which can greatly enlarge the application range of these outstanding piezoelectric single crystals.

Acknowledgments

This work was financially supported by the Ministry of Science and Technology of China through 863 Program (no. 2008AA03Z410) and 973 Program (no. 2009CB623305), the Natural Science Foundation of China (Nos. 60837003, 50777065 and 50602047), Shanghai Municipal Government (no. 08JC1420500), the Innovation Fund of Shanghai Institute of Ceramics (no. O99ZC4140G), and the Fund of National Engineering Research Center for Optoelectronic Crystalline Materials (no. 2005DC105003-2007K05).

References

[1] R.E. Service, Science 275 (1997) 1878.
[2] H.S. Luo, G.S. Xu, P.C. Wang, Z.W. Yin, Ferroelectrics 231 (1999) 97.
[3] S.E. Park, T.R. Shrout, J. Appl. Phys. 82 (1997) 1804.
[4] F.F. Wang, L.H. Luo, D. Zhou, X.Y. Zhao, H.S. Luo, Appl. Phys. Lett. 90 (2007) 212903.
[5] C.S. Hong, S.Y. Chu, W.C. Su, R.C. Chang, H.H. Nien, Y.D. Juang, J. Alloys Compd. 460 (2008) 658.
[6] K.G. Webber, R. Zuo, C.S. Lynch, Acta Mater. 56 (2008) 1219.
[7] X. Wen, C. Feng, L. Chen, S. Huang, Ceram. Int. 33 (2007) 815.
[8] Z. Yang, X. Chao, R. Zhang, Y. Chang, Y. Chen, Mater. Sci. Eng. B 138 (2007) 277.
[9] D.B. Lin, Z.R. Li, F. Li, Z. Xu, X. Yao, J. Alloys Compd. 489 (2010) 115.
[10] C.L. Huang, J.J. Wang, B.J. Li, W.C. Lee, J. Alloys Compd. 461 (2008) 440.
[11] S.J. Park, H.Y. Park, K.H. Cho, S. Nahm, H.G. Lee, D.H. Kim, B.H. Choi, Mater. Res. Bull. 43 (2008) 3580.
[12] C.L. Huang, Y.B. Chen, C.F. Tasi, J. Alloys Compd 460 (2008) 675.
[13] B.J. Fang, R.B. Sun, Y.J. Shan, K. Tezuka, H. Imoto, J. Phys. Chem. Solids 70 (2009) 893.
[14] S. Wongsaenmai, S. Ananta, R. Yimnirun, J. Alloys Compd. 474 (2009) 241.
[15] J. Luo, W. Hackenberger, S.J. Zhang, T.R. Shrout, IEEE Ultrasonic Symposium (IEEE), 2008, p. 261.
[16] M. Pham-Thi, C. Augier, H. Dammak, P. Gaucher, Ultrasonics 44 (2006) e267.
[17] S.J. Zhang, J. Luo, W. Hackenberger, N.P. Sherlock, R.J. Meyer Jr., T.R. Shrout, J. Appl. Phys. 105 (2009) 104506.
[18] M. Jin, J.Y. Xu, S.J. Fan, M.L. Shi, Integr. Ferroelectr. 96 (2007) 82.
[19] H.S. Luo, G.S. Xu, H.Q. Xu, P.C. Wang, Z.W. Yin, Jpn. J. Appl. Phys. 39 (2000) 5581.
[20] P. Yu, F.F. Wang, D. Zhou, W.W. Ge, X.Y. Zhao, H.S. Luo, J.L. Sun, X.J. Meng, J.H. Chu, Appl. Phys. Lett. 95 (2008) 252907.

[21] P. Sun, Q.F. Zhou, B.P. Zhu, D.W. Wu, C.H. Hu, J.M. Cannata, J. Tian, P.D. Han, G.F. Wang, K.K. Shung, IEEE Trans. Ultrason. Ferr. 56 (2009) 2760.
[22] Q.F. Zhou, B.P. Zhu, D.W. Wu, C.H. Hu, J.M. Cannata, J. Tian, P.D. Han, K.K. Shung, IEEE Ultrason. Symp. (2008) 1433.
[23] IEEE Standard on Piezoelectricity (IEEE New York), ANSI/IEEE Report No. 176–1987, 1987.
[24] J.H. Yin, W.W. Cao, J. Appl. Phys. 87 (2000) 7438.
[25] T. Liu, C.S. Lynch, Acta Mater. 51 (2003) 407.
[26] Y. Lu, D.Y. Jeong, Z.Y. Cheng, Q.M. Zhang, H.S. Luo, Z.W. Yin, D. Viehland, Appl. Phys. Lett. 78 (2001) 3109.
[27] X.Z. Liu, S.J. Zhang, J. Luo, T.R. Shrout, W.W. Cao, J. Appl. Phys. 106 (2009) 074112.
[28] R. Zhang, B. Jiang, W.H. Jiang, W.W. Cao, Appl. Phys. Lett. 89 (2006) 242908.